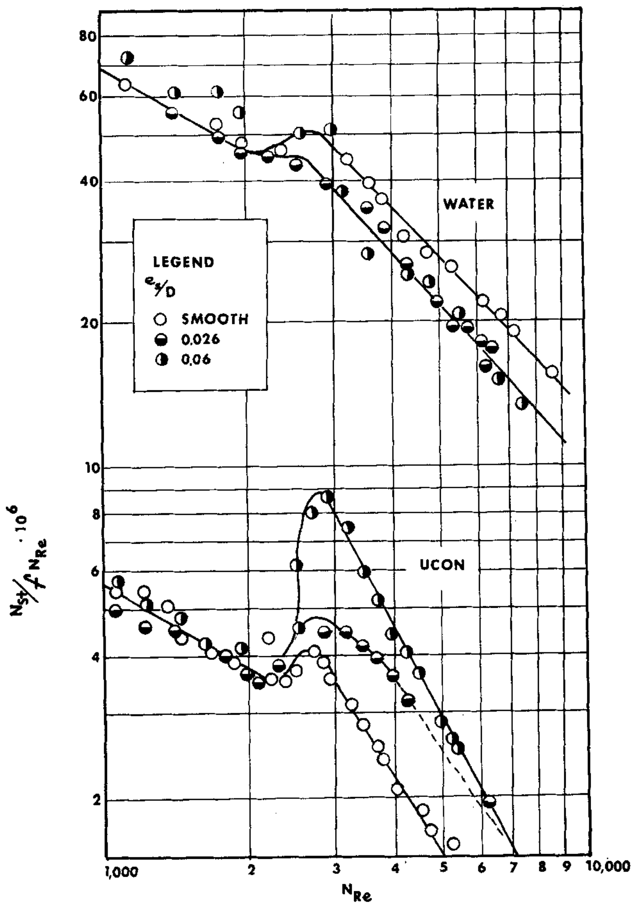

Fig. 3. Heat transfer efficiency for smooth and rough pipes.

His equation does not provide the Stanton number with a Prandtl number dependence. Consequently, the present experimental results for Ucon are an order of magnitude smaller than the predicted results of Sams' equation.

Heat transfer efficiency can be represented by the dimensionless group $N_{St}/f\,N_{Re}$, which is equivalent to the heat transmission per unit pressure drop. Figure 3 shows the variation of this group with the Reynolds number for all the tubes and fluids used in the investigation. As reported previously (*1* to *3*), the smooth tube was more efficient than either of the rough tubes when water was used as the test fluid. However, in the case of Ucon, the rough tubes are significantly more efficient in the transition-turbulent region. This difference in behavior holds whether the true surface area or the effective smooth surface is used to calculate the heat transfer coefficient. The increase in surface area for the roughest tube does not exceed 28%, whereas the increase in efficiency over that in the smooth tube is never less than 200% in the region studied.

It can be shown from boundary-layer theory that a smooth tube will eventually become more efficient than a rough one as the Reynolds number is increased, regardless of the Prandtl number of the fluid. However, the larger the Prandtl number the higher the Reynolds number must be in order for this to happen. Therefore in practice this fact is not important because very high Reynolds numbers are exceedingly difficult to obtain with viscous and consequently high-Prandtl-number fluids.

The work is now being extended to cover a wider range of Reynolds and Prandtl numbers in tubes with different roughness patterns.

NOTATION

f = friction factor
e_s/D = equivalent sand roughness
e/D = measured roughness
N_{Nu} = Nusselt number
N_{Pr} = Prandtl number
N_{Re} = Reynolds number
N_{St} = $h/\rho u c_p$ = Stanton number

LITERATURE CITED

1. Dipprey, D. F., and R. H. Sabersky, *Intern. J. Heat Mass Transfer,* **6**, 329-353 (1963).
2. Cope, W. F., *Proc. Inst. Mech. Engrs.,* **145**, 99 (1941).
3. Hastrup, R. C., *Jet Propulsion,* 259 (April, 1958).
4. McAdams, W. H., "Heat Transmission," p. 241, McGraw-Hill, New York (1954).
5. Sams, E. W., *Natl. Advisory Committee Aeron. RM E52 D17* (1952).
6. Perry, R. H., "Chemical Engineers' Handbook," 4 ed., pp. 5-20, McGraw-Hill, New York (1963).

Diffusion with Consecutive Heterogeneous Reactions

J. L. HUDSON
University of Illinois, Urbana, Illinois

Irreversible first-order heterogeneous chemical reaction on the wall of a tube in which a fluid is flowing in fully developed laminar flow has been studied by several investigators (*1, 2*). In this note the problem will be extended to the case of consecutive reactions. The analysis parallels that of Wissler and Schechter (3), who treated consecutive irreversible first-order homogeneous reactions.

Consider the heterogeneous reactions

$$A_1 \rightarrow \beta A_2 \rightarrow \text{products} \qquad (1)$$

The concentrations are taken to be dilute and fluid properties are assumed constant. A plug flow velocity profile will be used, although a similar treatment could be used for the Poiseuille distribution. Under these restrictions the dimensionless material balance on component 1 is

$$\frac{1}{y}\frac{\partial}{\partial y}y\frac{\partial C_1}{\partial y} = \frac{\partial C_1}{\partial x} \qquad (2)$$

with boundary conditions

$$x = 0 \qquad C_1 = 1$$
$$y = 0 \qquad C_1 = \text{finite}$$
$$y = 1 \qquad \frac{\partial C_1}{\partial y} = -K_1C_1$$

The solution to this system is

$$C_1 = \sum_i a_i e^{-\lambda_i^2 x} J_o(\lambda_i y) \qquad (3)$$

where

INFORMATION RETRIEVAL*

Peak nucleate boiling fluxes for liquid oxygen on a flat horizontal platinum surface at buoyancies corresponding to accelerations between −0.03 and 1g_E, Lyon, D. N., M. C. Jones, G. L. Ritter, C. A. Chiladakis, and P. G. Kosky, **A.I.Ch.E. Journal, 11,** No. 5, p. 773 (September 1965).

Key Words: A. Nucleate Boiling Fluxes-8, 7, Oxygen-9, Heat Transfer-8, 7, Nucleate Boiling-9, 8, Gravity-6, Boiling-9, 8,

Abstract: Peak nucleate boiling fluxes for liquid oxygen near one atmosphere have been measured on a flat polished horizontal platinum surface located in a known variable magnetic-field gradient that produced steady accelerations (which could be maintained indefinitely) on the oxygen acting in opposition to the earth's gravitation, g_E. Measurements were made under conditions ranging from net negative (directed away from the heated surface) accelerations to the normal acceleration, 1.0 g_E.

Thermodynamic consistency tests for solid-liquid equilibria, Null, Harold R., **A.I.Ch.E. Journal, 11,** No. 5, p. 780 (September, 1965)

Key Words: A. Testing-8, Solid-Liquid Equilibria-8, 9, Phase Equilibria-8, 9, Thermodynamic Consistency Tests-10, Indium Antimonide-9, Gallium Antimonide-9, Sodium Carbonate-9, Sodium Sulfate-9,

Abstract: The problems associated with thermodynamic consistency tests are discussed, and a new technique for evaluating the validity of solid-liquid equilibria has been developed. Several possible test equations are presented and applied to test the consistency of three sets of solid-liquid equilibrium data.

Gas absorption in a fin-wall conduit, Sweeney, Thomas L., and Seymour Calvert, **A.I.Ch.E. Journal, 11,** No. 5, p. 785 (September, 1965).

Key Words: A. Air-5, Ammonia-5, Oxygen-5, Water-5, Gas Rate-6, Liquid Rate-6, Pressure Drop-7, 8, Flooding-7, Friction Factor-7, End Effects-7, Loading-7, Height of a Transfer Unit-7, Absorption-8, Desorption-8, Mass Transfer-8, Baffles-10, Fins-10, Fin-Wall Conduit-10, Scrubber-10. B. Flow Patterns-9, Water-5, Fin-Wall Conduit-10.

Abstract: The purpose of this paper is to present mass transfer and pressure drop characteristics of the fin-wall conduit. The fin-wall conduit is a rectangular duct with transverse fins attached to one or more internal walls. Desorption of oxygen from water and absorption of ammonia into water were studied. The equipment utilized in this study consisted of four experimental conduits. The columns were rectangular conduits formed by two fin-walls (aluminum) and two smooth walls (transparent plastic).

(Continued on page 946)

* For details on the use of these Key Words and the A.I.Ch.E. Information Retrieval Program, see **Chem. Eng. Progr.,** Vol. 60, No. 8, p. 88 (August, 1964). A free copy of this article may be obtained by sending a post card, with the words "Key Word Article" and your name and address (please print) to Publications Department, A.I.Ch.E., 345 East 47 St., N. Y. N. Y., 10017. Price quotations for volume quantities on request. Free tear sheets of the information retrieval entries in this issue may be obtained by writing to the New York office.

$$a_i = \frac{2\,J_1(\lambda_i)}{\lambda_i[J_o^2(\lambda_i) + J_1^2(\lambda_i)]}$$

and λ_i are the roots of

$$\lambda\,J_1(\lambda) - K_1 J_o(\lambda) = 0$$

The dimensionless material balance on component 2 is

$$\frac{1}{y}\frac{\partial}{\partial y}y\frac{\partial C_2}{\partial y} = \alpha\frac{\partial C_2}{\partial y} \qquad (4)$$

with boundary conditions

$x = 0 \qquad C_2 = \gamma$

$y = 0 \qquad C_2 = \text{finite}$

$y = 1 \qquad -\dfrac{\partial C_2}{\partial y} = \alpha K_2 C_2 - \alpha\beta K_1 C_1$

Equation (4) is homogeneous but has a nonhomogeneous boundary condition at $y = 1$. It is, therefore, convenient to introduce

$$\eta = C_2 - \frac{K_1}{K_2}\beta\sum_i a_i e^{-\lambda_i^2 x} J_o(\lambda_i) \quad (5)$$

The equation now becomes

$$\frac{1}{y}\frac{\partial}{\partial y}y\frac{\partial\eta}{\partial y} = \alpha\frac{\partial\eta}{\partial x} - \frac{K_1}{K_2}\alpha\,\beta \sum_i a_i\lambda_i^2 e^{-\lambda_i^2 x} J_o(\lambda_i) \quad (6)$$

with boundary conditions

$$x = 0 \qquad \eta = \gamma - \frac{K_1}{K_2}\beta\sum_i a_i J_o(\lambda_i) = \gamma - \frac{K_1}{K_2}\beta$$

$y = 0 \qquad \eta = \text{finite}$

$y = 1 \qquad -\dfrac{\partial\eta}{\partial y} = \alpha K_2\eta$

A solution to Equation (6) is

$$\eta = \sum_j b_j(x) J_o(\mu_j y) \qquad (7)$$

where the $b_j(x)$ are as of yet undetermined functions of x. The $Y_o(\mu_j y)$ solution is discarded since it is infinite at $y = 0$. From the boundary condition at $y = 1$, the eigenvalues μ_j are found to be the roots of

$$\mu J_1(\mu) - \alpha K_2 J_o(\mu) = 0 \qquad (8)$$

Equation (7) is substituted into Equation (6), and because of the orthogonality properties of the Bessel functions, the result is multiplied by $yJ_o(\mu_j y)dy$ and integrated from 0 to 1, yielding

$$b_j'(x) + \frac{\mu_j^2}{\alpha}b_j(x) = \beta\frac{K_1}{K_2}\,\frac{2\,J_1(\mu_j)}{\mu_j[J_o^2(\mu_j) + J_1^2(\mu_j)]}$$

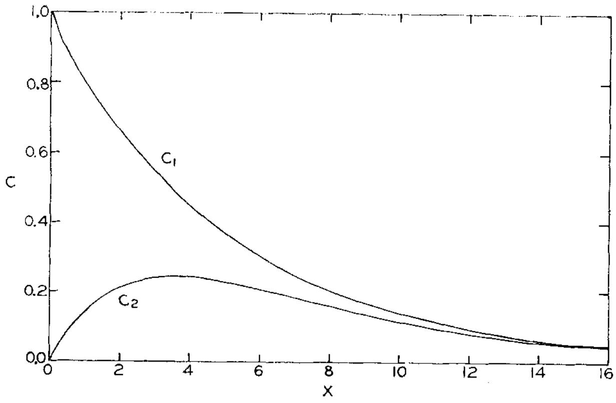

Fig. 1. Average concentration as a function of axial position.

$$\sum_i a_i \lambda_i^2 e^{-\lambda_i^2 x} J_o(\lambda_i) \qquad (9)$$

where the prime indicates differentiation. The solution to (9) is the sum of the solution to the homogeneous equation and the particular solution, or

$$b_j(x) = d_j e^{\frac{-\mu_j^2 x}{\alpha}} + \frac{2\beta K_1 J_1(\mu_j)}{K_2[J_o^2(\mu_j) + J_1^2(\mu_j)]} \sum_i a_i\lambda_i^2 J_o(\lambda_i) \frac{e^{-\lambda_i^2 x}}{\left(\frac{\mu_j^2}{\alpha} - \lambda_i^2\right)} \qquad (10)$$

where d_j are constants to be determined. The boundary condition at $x = 0$ is

$$\gamma = \frac{K_1}{K_2}\beta + \sum_j b_j(0)\, J_o(\mu_j y) \qquad (11)$$

The constants d_j are found by multiplying (11) by $y\,J_o(\mu_j y)dy$ and by integrating from 0 to 1. With the d_j determined, the $b_j(x)$ are known from (10) and the solution is seen to be

$$C_2 = \frac{K_1}{K_2}\beta \sum_j a_j\, J_o(\lambda_j)\, e^{-\lambda_j^2 x} + \sum_j \frac{2\,J_o(\mu_j y)\, J_1(\mu_j)}{\mu_j[J_o^2(\mu_j) + J_1^2(\mu_j)]} \cdot \left\{ \left(\gamma - \frac{K_1}{K_2}\beta\right) e^{\frac{-\mu_j^2 x}{\alpha}} + \frac{K_1}{K_2}\beta \sum_i \frac{a_i\lambda_i^2 J_o(\lambda_i)}{\left[\frac{\mu_j^2}{\alpha} - \lambda_i^2\right]} \left(e^{-\lambda_i^2 x} - e^{-\mu_j^2 x/\alpha}\right) \right\} \qquad (12)$$

The average concentration in the tube as a function of axial position is

$$\bar{C}_n(x) = 2\int_0^1 y\, C(y, x)\, dy \quad n = 1, 2$$

These averages are shown in Figure 1 for $K_1 = 0.1$, $K_2 = 0.2$, $\gamma = 0$, $\beta = 1$, and a diffusivity ratio $\alpha = 0.5$. As is expected, the concentration of component 2 reaches a maximum before falling to zero.

NOTATION

c_n	= concentration, $n = 1, 2$
c_{no}	= inlet concentration
C_n	= c_n/c_{10}
D_n	= diffusivity
k_n	= reaction rate constant
K_n	= k_nR/D_1
r	= radial position
R	= tube radius
V	= fluid velocity
x	= D_1z/R^2V
y	= r/R
z	= axial position

Greek Letters

α	= D_1/D_2
β	= stoichiometric coefficient
γ	= c_{20}/c_{10}
λ_i, μ_j	= eigenvalues
η	defined by Equation (5)

LITERATURE CITED

1. Baron, Thomas, W. R. Manning, and H. F. Johnstone, *Chem. Eng. Progr.*, **48**, 125 (1952).
2. Katz, S., *Chem. Eng. Sci.*, **10**, 202 (1959).
3. Wissler, E. H., and R. S. Schechter, *App. Sci. Res.*, **A10**, 198 (1961).

Predicting Vertical Film Flow Characteristics in the Entrance Region

DUANE F. BRULEY

Clemson University, Clemson, South Carolina

Liquid films flowing over vertical surfaces under the influence of gravity are encountered in many types of heat and mass transfer equipment: distillation columns, evaporators, wetted wall columns. Therefore, a complete understanding of film flow, from the entrance to the exit, should be of interest industrially, experimentally, and academically.

Many papers concerning film flow have been published since the early 1900's. However, there is still much to be learned before precise design calculations can be carried out for operations involving this flow phenomenon. Dunkler and Bergelin (2) discussed the importance of understanding the mechanics of film flow to the analysis of performance of industrial equipment. The authors pointed out that it is necessary to know the exact area for mass or heat transfer so that a combined coefficient *ka* is not required for design purposes. The mass transfer coefficient *k* and the area for transfer *a* are independent functions and should be treated as such if a rational analysis is to be made.

Although many experimental methods (*1, 3, 4, 6*) have been used to determine film thicknesses, most of the investigations have been done in the